Earth and Planetary Science Letters 391 (2014) 193–200

Contents lists available at ScienceDirect

Earth and Planetary Science Letters

www.elsevier.com/locate/epsl

Comparison of hydrological responses to the Wenchuan and Lushan earthquakes

Zheming Shi [a,b], Guangcai Wang [a,*], Chi-yuen Wang [b], Michael Manga [b], Chenglong Liu [c]

[a] School of Water Resources and Environment, China University of Geosciences, Beijing 100083, China
[b] Department of Earth and Planetary Science, University of California, Berkeley, CA 94720, USA
[c] Institute of Geology, China Earthquake Administration, Beijing 100029, China

ARTICLE INFO

Article history:
Received 25 October 2013
Received in revised form 26 January 2014
Accepted 30 January 2014
Available online xxxx
Editor: P. Shearer

Keywords:
Wenchuan earthquake
Lushan earthquake
groundwater level
liquefaction
static strain
permeability

ABSTRACT

On 20th April, 2013, a large earthquake (Lushan M_w 6.6) occurred in Sichuan, China, in the same fault zone as the devastating 2008 M_w 7.9 Wenchuan earthquake. The two earthquakes have similar focal mechanisms and both caused large hydrological changes in the region. The similarity of focal mechanisms, fault zone geology and the abundance of hydrological responses provide a rare opportunity for testing proposed mechanisms for hydrological responses to earthquakes. Using data from wells installed in hard rocks, we find that both the magnitude and the sign of water level changes are inconsistent with those predicted by the coseismic strain hypothesis in the near-field and in the intermediate-field. Instead, permeability change may be the dominant mechanism for the coseismic changes in water level. We also find that the minimum seismic energy required to trigger liquefaction for the Wenchuan earthquake is only 1/20 of that for the Lushan earthquake, suggesting either that the occurrence of liquefaction is more sensitive to low seismic frequencies or that the Wenchuan earthquake changed the sensitivity of unconsolidated materials, and properties had not completely recovered during the 5-year interval between the two earthquakes.

1. Introduction

Earthquake-induced hydrological changes have been documented for thousands of years (e.g., Institute of Geophysics – CAS, 1976). However, instrumental records of these changes have become available only in the last few decades. Several mechanisms have been proposed to explain the hydrological changes, including elastic static strain caused by slip on the ruptured fault (Ge and Stover, 2000; Muir-Wood and King, 1993; Wakita, 1975), undrained consolidation (Wang, 2001), liquefaction (Manga et al., 2003; Roeloffs, 1998) and permeability changes (Brodsky et al., 2003; Elkhoury et al., 2006; Rojstaczer et al., 1995; Wang et al., 2004; Xue et al., 2013). Many of these previous studies used data from wells in unconsolidated sediments (Roeloffs, 1998; Rojstaczer et al., 1995; Sil and Freymueller, 2006; Wang, 2001; Wang and Chia, 2008) and only a few studies are based on measurements in hard rocks in the near field (Jónsson et al., 2003; Zhang and Huang, 2011). Furthermore, identifying the dominant mechanism(s) for observed responses is often difficult because observations are limited to a single earthquake. Comparison of responses to multiple earthquakes with similar focal mechanisms occurring on the same fault zone may thus be useful for testing hypotheses.

An ideal case is provided by the occurrence of the large (M_w 6.6) Lushan earthquake on 20th April, 2013, in Sichuan, China, nearly five years after the devastating M_w 7.9 Wenchuan earthquake. The two earthquakes have the same thrust focal mechanism (Fig. 1) and occurred on the same fault (the Longmenshan fault). Both earthquakes caused large hydrological changes. The similarity of focal mechanisms and fault zone geology eliminates one of the variables in comparing the hydrological responses to different earthquakes. The abundance of hydrological responses provides an excellent opportunity for testing the proposed mechanisms for hydrological responses.

Here we report two types of hydrological response, i.e., coseismic water-level change and liquefaction occurrence, following the two earthquakes. We then analyze and compare the co-seismic responses, which allow us to assess mechanisms responsible for the hydrological changes.

2. Geological setting

Both the Wenchuan and Lushan earthquakes are located in the Longmenshan fault zone (Fig. 1) along the eastern margin of the

* Corresponding author. Tel.: +86 10 82323125; fax: +86 10 82321081.
E-mail address: wanggc@pku.edu.cn (G. Wang).

http://dx.doi.org/10.1016/j.epsl.2014.01.048
0012-821X/

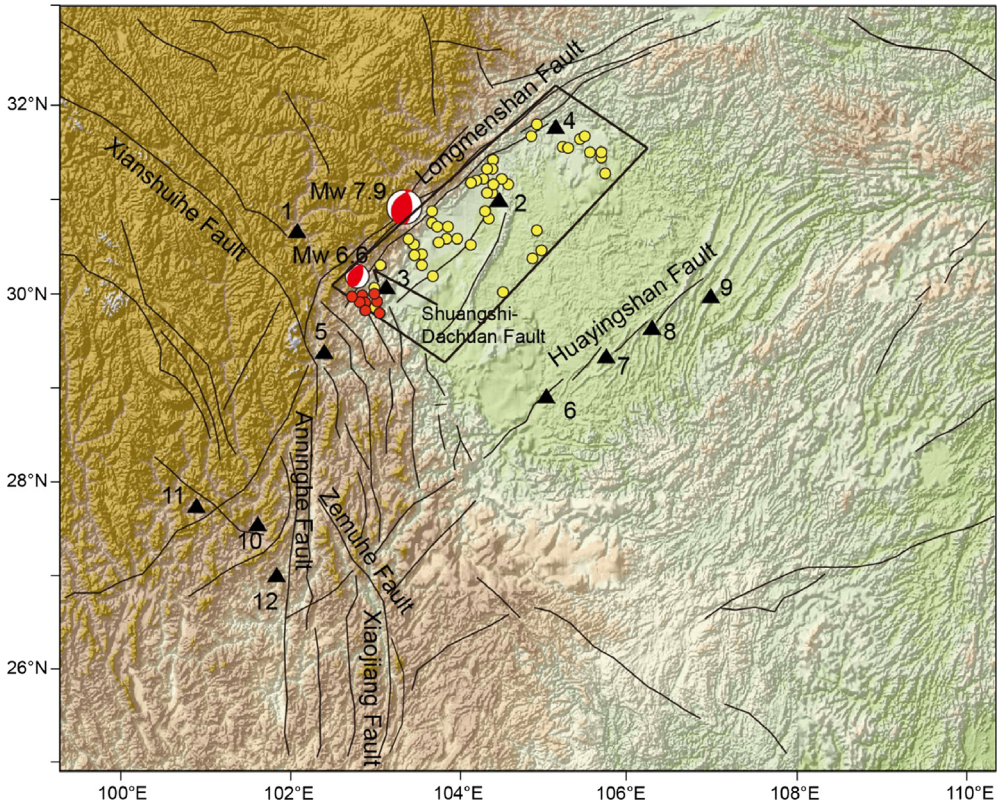

Fig. 1. Geological setting and locations of the groundwater monitoring wells (black triangles) and epicenters of the Wenchuan (M_w 7.9) and Lushan (M_w 6.6) earthquakes. Beach balls show the lower hemisphere projection of the focal mechanism. Black lines show mapped faults. The yellow and red circles show the locations of liquefaction phenomena following the Wenchuan and Lushan earthquakes, respectively. [Liquefaction sites following the Wenchuan earthquake are obtained from Yuan et al. (2009); Cao et al. (2010). The liquefaction sites after the Lushan earthquake are obtained from the report of Institute of Geology, China Earthquake Administration (CEA); The institute of Crustal Dynamic, CEA; Liu and Huang (2013); Zhang et al. (2013)]. (For interpretation of the references to color in this figure legend, the reader is referred to the web version of this article.)

Tibet Plateau. The fault zone strikes NE to SW with a length of 500 km, and a width of about 40–50 km. Prior to the Wenchuan earthquake, there was only one historical earthquake with $M > 6$ on this fault (1989, M_w 6.1). The M_w 7.9 Wenchuan earthquake produced a unilateral 340 km-long rupture, with thrust and right-lateral components on a high-angle fault dipping to the NW (Wang et al., 2011; Xu et al., 2009). The Lushan earthquake occurred ~85 km southwest of the Wenchuan earthquake with a focal mechanism dominated by a thrust fault component. The ruptured length is about 66.5 km along the strike of the Longmenshan fault zone (Liu et al., 2013).

We define epicentral distances within about 1.5 rupture fault lengths as the near-field, with the intermediate-field spanning distances between 1.5 to 10 ruptured fault lengths. Thus, the near-field for Wenchuan and Lushan events are distances less than 500 km and 90 km, respectively, from their respective epicenters. In order to compare the hydrological responses following the two earthquakes, we select a study area within 500 km of the Wenchuan epicenter (Fig. 1). This region is in the near-field of the Wenchuan earthquake but includes both the near-field and the intermediate-field of the Lushan earthquake.

3. Data collection

Monitoring the dynamics of subsurface fluids is an important part of the earthquake prediction program in China, which began in the 1960s. A nationwide monitoring network documents groundwater level, water temperature, and radon (Rn) and mercury (Hg) in groundwater. Monitoring sites are distributed along active faults or points of special tectonic interest (Huang et al., 2004). Because of the smaller magnitude of the Lushan earthquake, the influence region is mainly in the Sichuan and Chongqing areas. For the present study we focus on the monitoring wells located in Sichuan and Chongqing areas to compare and contrast the co-seismic responses to the two earthquakes.

Data sampling and availability are not uniform. Because of the different digital logging of these monitoring wells, the sampling rates are either 1 min or 1 h. Some wells have transducers to measure both water level and temperature while some only measure the water level. In addition, some wells that worked well during the Wenchuan earthquake were abandoned before the 2013 Lushan earthquake, while some new wells were built after the Wenchuan earthquake. Here, we only analyze data from wells that recorded the effects of both earthquakes. In total we collected data from 12 wells located along Longmenshan, Huayingshan and Anninghe faults (Fig. 1). Depths range from 69 to 4076 m, and epicenter distances range from 95 to 510 km to the Wenchuan epicenter and 29 to 438 km to the Lushan epicenter. Most wells are in consolidated sandstone and two wells are in fractured granite (Table 1).

A research group was organized by the China Earthquake Administration to investigate liquefaction phenomena after the Wenchuan earthquake. This is a comprehensive liquefaction survey and our liquefaction data are obtained from their study (Cao et al., 2010; Yuan et al., 2009). After the Lushan earthquake, four research groups (Institute of Geology, China Earthquake Administration (CEA); The Institute of Crustal Dynamic, CEA; Chinese Academy of Geological Sciences and Chengdu University of Technology) made independent field surveys immediately after the earthquake. Their investigations included the entire disaster area

Table 1
Features of the groundwater monitoring wells.

Well number	Sample rate	Lithology	Depth [m]	Wenchuan earthquake		Lushan earthquake	
				Epicenter distance [km]	e[a] [J m^{-3}]	Epicenter distance [km]	e[a] [J m^{-3}]
1	1 min	Metasandstone	100	95	18	98	8.0×10^{-1}
2	1 min	Sandstone	3072	103	14.2	165	4.3×10^{-2}
3	1 min	Sandstone	175	111	11.2	29	8.4
4	1 h/1 min	Sandstone	4076	157	3.9	239	1.5×10^{-2}
5	1 h	Granite	968	204	1.8	117	1.2×10^{-1}
6	1 min	Quartzite	101	267	7.9×10^{-1}	237	1.5×10^{-2}
7	1 min	Sandstone	251	272	0.7	269	1.0×10^{-2}
8	1 min	Sandstone	300	284	0.5	290	7.8×10^{-3}
9	1 min	Mudstone and sandstone	105	328	1	347	1.1×10^{-2}
10	1 min	Mudstone and sandstone	109	432	0.6	350	7.6×10^{-3}
11	1 min	Gravel	69	435	0.2	353	4.5×10^{-3}
12	1 min	Granite	200	510	0.2	438	4.4×10^{-3}

[a] e in the table represents the seismic energy density, it is calculated from $\log(r) = 0.48M - 0.33\log e(r) - 1.4$ (Wang, 2007). Where r is the actual epicenter distance in km, M is the magnitude of the earthquake and e refers to the seismic energy density in (J m^{-3}).

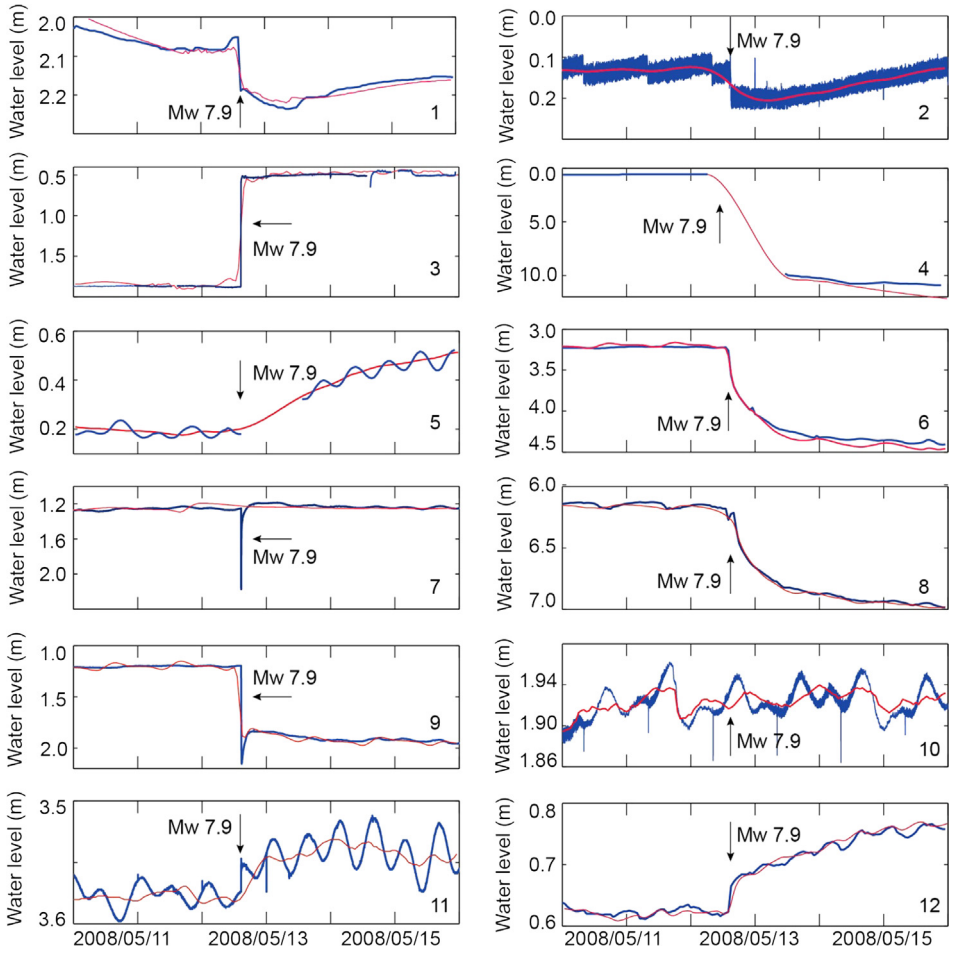

Fig. 2. Water level fluctuations before and after the Wenchuan earthquake. The blue curves show the original groundwater level changes while the red curves show the corrected water level with tidal signal removed. (For interpretation of the references to color in this figure legend, the reader is referred to the web version of this article.)

(Liu and Huang, 2013; Zhang et al., 2013). The liquefaction data in our study are obtained from all four groups. Nevertheless, the completeness of the mapping in these studies and ability to identify the maximum distance over which liquefaction occurred are impossible to assess. However, as the objective of all of these studies was a comprehensive assessment of liquefaction, we assume their reports are complete.

4. Co-seismic hydrological response caused by the Wenchuan and Lushan earthquake

4.1. Co-seismic water level changes in response to the Wenchuan and Lushan earthquake

Groundwater levels in some wells show a clear response to earth tides (Fig. 2, Fig. 3). We use the program Baytap-G

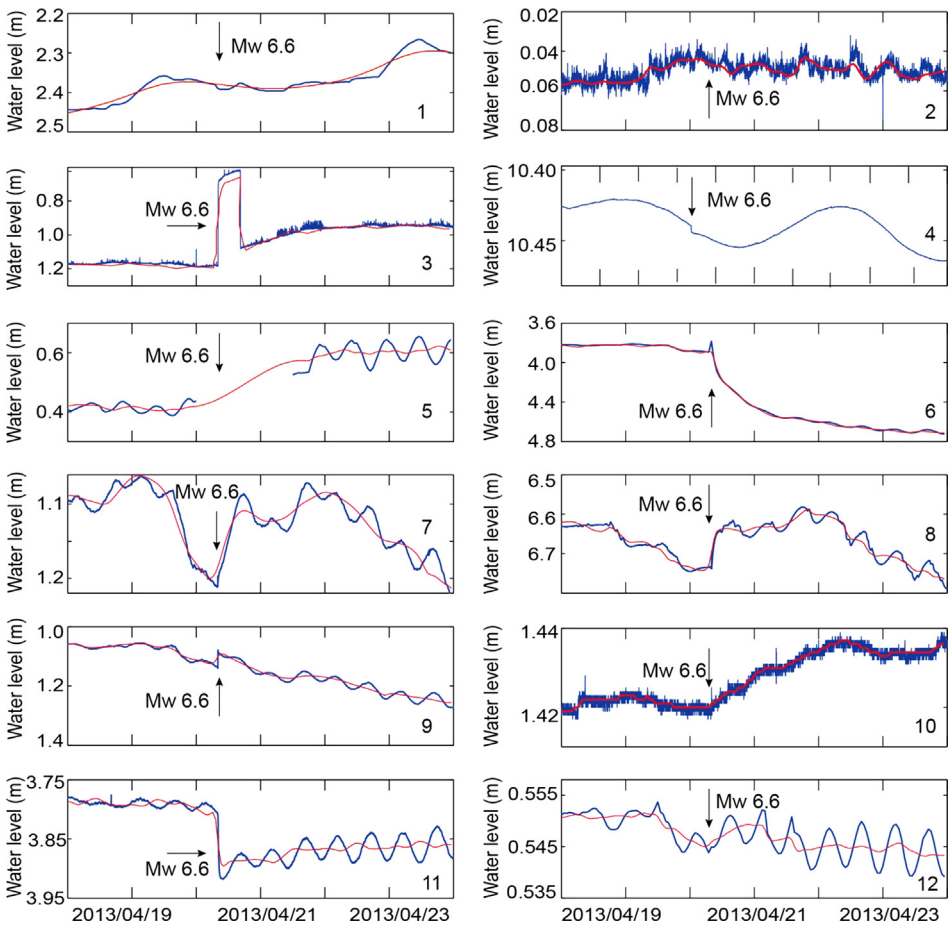

Fig. 3. Water level fluctuations before and after the Lushan earthquake. The blue curves show the original groundwater level changes while the red curves show the corrected water level with tidal signal removed. (For interpretation of the references to color in this figure legend, the reader is referred to the web version of this article.)

(http://ggjapan.miz.nao.ac.jp/baytap/uncompress), that incorporates a Bayesian inversion process (Burbey, 2010; Tamura et al., 1991), to remove tidal effects. Fig. 2 and Fig. 3 show both the original and the tidally-corrected data. The water levels in the monitoring wells have large co-seismic responses to the two earthquakes (up to 9.188 m and 0.752 m, respectively). For the Wenchuan earthquake, all 12 wells show large co-seismic changes in water level except for well #10 (Fig. 2). Combining Figs. 1 and 2, we can identify systematic patterns in the responses. Water level declined in wells are located on the two sides of the Longmenshan fault (#1, #2, #4) and Huayingshan fault (#6, #7, #8, and #9), which is parallel to the Longmenshan fault. Water levels rose in wells along the strike of the Longmenshan fault, #3, #5, #11 and #12 (Shi et al., 2013).

For the Lushan earthquake, 9 of the 12 wells show co-seismic water level changes. Wells #1, #2 and #12 show no co-seismic changes in water level (Fig. 3). Comparing the water level changes for the two earthquakes, only wells #3, #4, #5, #6 show the same sign of co-seismic changes, while wells #7, #8, #9, and #11 have opposite sign of water level changes. Well #10, which did not respond to the Wenchuan earthquake, showed a rise in water level following the Lushan earthquake. As summarized in Table 2, we see that the amplitudes of water level changes after the Wenchuan earthquake are generally larger than those after the Lushan earthquake except wells #10 and #11.

For both earthquakes, there is no clear relationship with the epicentral distance or the response amplitude, both in the near-field and in the intermediate-field (Fig. 4a).

Table 2
Co-seismic changes of water level following the Wenchuan and Lushan earthquake.

Well number	Wenchuan earthquake		Lushan earthquake	
	Water level change	Amplitude [m]	Water level change	Amplitude [m]
1	Step drop	−0.14	–	–
2	Step drop	−0.063	–	–
3	Step rise	1.2	Step rise	0.52
4	Step drop	−9.188	Step drop	−0.005
5	Gradual rise	0.269	Gradual rise	0.14
6	Gradual drop	−1.1	Gradual drop	−0.752
7	Step drop	−0.92	Gradual rise	0.1
8	Gradual drop	−0.68	Gradual rise	0.101
9	Step drop	−0.95	Step rise	0.042
10	–	–	Gradual rise	0.002
11	Step rise	0.034	Step drop	−0.086
12	Step rise	0.05	–	–

Note: – indicates no co-seismic changes.

4.2. Liquefaction

After the Wenchuan earthquake, widespread liquefaction phenomena occurred in the Sichuan basin, covering an area of 500 km in length and 200 km in width (Fig. 1). But the liquefaction distribution was not uniform, with most occurring in the rectangular area outlined in Fig. 1 (Yuan et al., 2009). The most distant liquefaction sites were observed in Suining to the east, Hanyuan country to the south and Longnan, Gansu province to the north (Cao et al., 2010). For the Lushan earthquake, on the other hand, liquefaction only occurred near river terraces and alluvial flats along the Shuangshi-Dachuan fault, a sub-fault of the Longmenshan fault

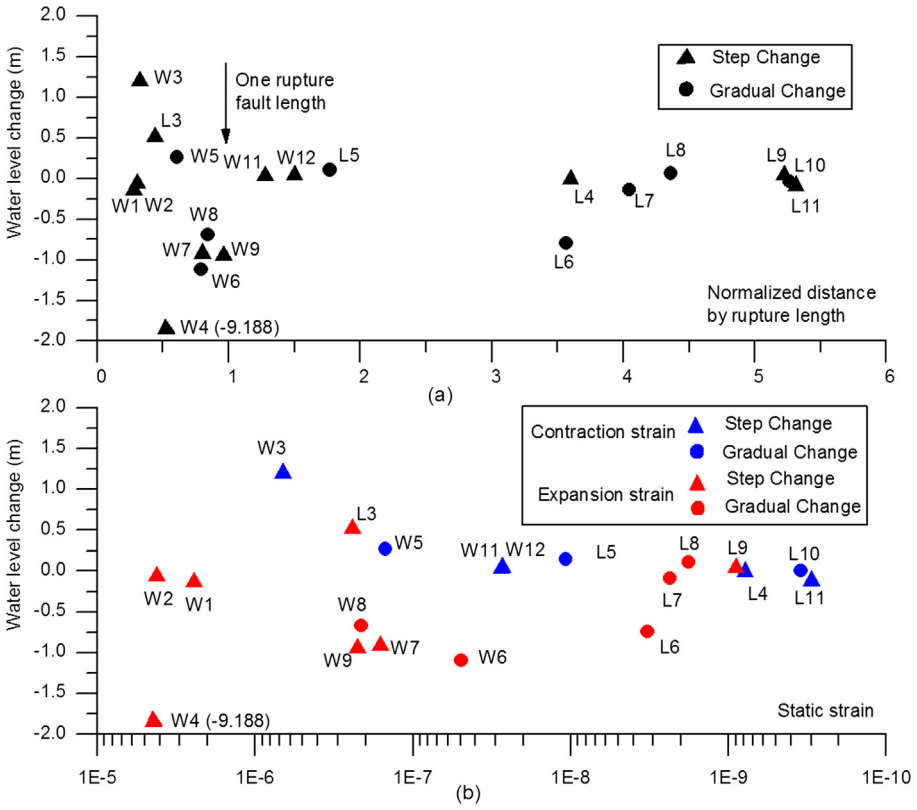

Fig. 4. Relationship between water level change, epicenter distance, and volumetric strain, following the two earthquakes. The triangles and circles in both figures indicate the step changes and gradual changes. The label "W" indicates the water level changes in response to the Wenchuan earthquake while the label "L" indicates the changes in response to the Lushan earthquake. (a) Water level changes versus epicenter distance (here, the epicenter distance is normalized by dividing it by the fault rupture length); (b) Water level changes versus static strain calculated from the dislocation model (blue indicates expansion and red indicates contraction). (For interpretation of the references to color in this figure legend, the reader is referred to the web version of this article.)

(Fig. 1). According to the field survey conducted by the four different institutions, the reported liquefaction phenomena occurred as far as 20 km away from the epicenter (reported from Institute of Geology, Institute of Crustal Dynamic, CEA; Liu and Huang, 2013; Zhang et al., 2013). Along the Shuanghe River at Shuangshi town, liquefaction formed a linear zone of sand and water ejections, with the same strike as the Longmenshan front Mountain fault zone (Zhang et al., 2013). Based on the global data set for earthquake-induced liquefaction, Wang (2007) found the threshold distance for different earthquake magnitudes. In our study, the maximum distance from the epicenter of the major liquefaction features for the Wenchuan earthquake is about 210 km, about ten times greater than the maximum distance of liquefaction for the Lushan earthquake. Using an empirical scaling relation from Wang (2007), we find that the minimum seismic energy density to trigger liquefaction in the Wenchuan earthquake is about 1.4 J/m^3, but is 20 times greater (~30 J/m^3) in the Lushan earthquake (in the absence of a better relationship, we apply the result in Wang (2007) to China).

5. Computing co-seismic strain and water level changes

5.1. Co-seismic static strain field calculated by the dislocation model

We use Coulomb 3.3 (Lin and Stein, 2004; Toda et al., 2005), based on Okada's elastic half space theory (Okada, 1985), to compute the co-seismic strain field caused by the earthquakes. For the Wenchuan earthquake, we use 31.100°N, 103.300°E as the location of the epicenter and the finite fault model obtained from the USGS, which consists of 168 sub-faults, each with a length of 15 km and a width of 5 km. Details are available at http://www.geol.ucsb.edu/faculty/ji/big_earthquakes/home.html. For Lushan earthquake, we assume the fault-plane solution of Liu et al. (2013) that consists of a single rupture plane striking 214°SW and dipping 38°SE, 66.5 km long along the strike and 35 km wide down dip, with an epicenter located at 30.314°N, 102.934°E and a hypocentral depth of 15 km.

5.2. Predicted magnitude of co-seismic water-level change from the static strain model

We compare the ratios of the observed water-level change and the volumetric strain, i.e., the strain sensitivity $A_s = \Delta h/\Delta\varepsilon_{kk}$, predicted from the theoretical volumetric strain and the well responses to tides (Itaba et al., 2008; Lai et al., 2010; Roeloffs, 1996). We use the tidal analysis program Baytap-G (Tamura et al., 1991) to estimate the tidal water level response and the program ETGTAB (http://www.bfo.geophys.uni-stuttgart.de/etgtab.html) to estimate the theoretical tidal volumetric strain. For estimating the tidal response we use the M_2 tide because of its larger amplitude and because it is less affected by the barometric pressure (Doan et al., 2006). We extract the amplitude of the M_2 component from 4 months of groundwater-level data before each earthquake. We estimate the coseismic water-level change predicted by the static strain model by combining the strain sensitivity, so computed, and the static strain from the dislocation model.

6. Result and discussion

6.1. Water-level changes

In the near-field, two mechanisms have typically been invoked to explain water level changes: (1) co-seismic static strain that

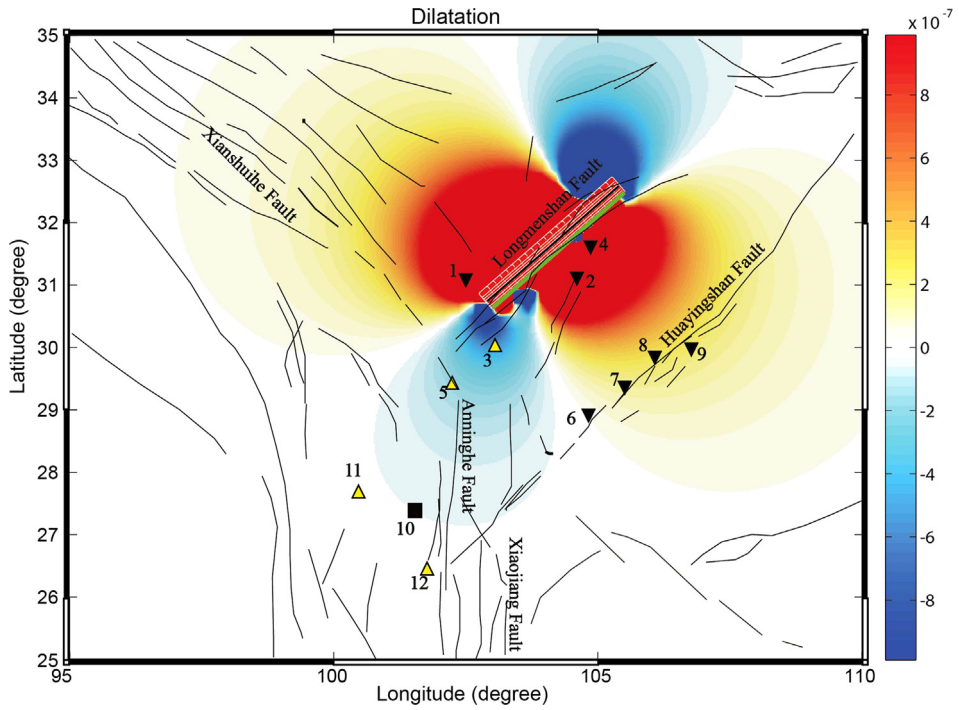

Fig. 5a. Co-seismic water level changes and co-seismic strain field, following the Wenchuan earthquake, calculated from the fault dislocation model. The blue zones show contraction while the red zones indicate dilation. Yellow triangles show wells with a co-seismic water level rise, while the black triangles show wells with a co-seismic water level decline. The black square indicates no co-seismic water-level changes. The black lines show mapped faults. (For interpretation of the references to color in this figure legend, the reader is referred to the web version of this article.)

changes pore pressure and hence water level (Ge and Stover, 2000; Jónsson et al., 2003), or (2) dynamic strains that induce consolidation (Wang, 2001; Wang and Chia, 2008). In the intermediate-field, permeability enhancement induced by dynamic stress is often considered the most plausible mechanism to explain water level changes (Brodsky et al., 2003; Elkhoury et al., 2006; Wang et al., 2009).

We begin by evaluating the mechanism of co-seismic static strain. If the model is correct, both the predicted sign and magnitude of the coseismic change of water level (Roeloffs, 1996) should agree with the observations. Using the fault dislocation model, we compute the co-seismic strain field caused by the Wenchuan and Lushan earthquakes (Figs. 5a, 5b). For Wenchuan earthquake, the wells located in the dilated zone all show a co-seismic decline of water level but a rise of water level in the zone with contraction. Thus the sign of water level changes agree with that predicted by the co-seismic static strain hypothesis. For Lushan earthquake, the direction of changes in water level are not consistent with the strain field (Fig. 5b). For example, wells #3 (the well #3 is close to the epicenter, so the water level changes may also be affected by fault complexities, step-overs, etc.), #7, #8 and #9 show rises in the zone of dilation. In addition, wells #4 and #11 show a decline in water level in the region of contraction. The inconsistency of water-level changes implies that the mechanism of co-seismic elastic strain is not the dominate mechanism either in the near-field or in the intermediate-field for the Lushan earthquake. Furthermore, there is no clear trend in the relationship between the magnitude of the coseismic volumetric strain and the water level-change for both earthquakes (Fig. 4b).

We next test the predicted magnitude of the coseismic water-level change from the static strain model. The comparison shows that the observed coseismic water-level changes are much greater than those predicted from the static strain model for both earthquakes (Table 3). This indicates that the static strain hypothesis is not the dominant mechanism causing water level changes, both in the near- and intermediate-field, contradicting the conclusion from a previous study (Zhang and Huang, 2011).

Furthermore, because the wells are all constructed in consolidated rocks, the mechanism of undrained consolidation does not apply in the present case. Thus, the only remaining proposed mechanism is permeability enhancement (Brodsky et al., 2003; Elkhoury et al., 2006; Rojstaczer et al., 1995; Wang et al., 2004). And the mechanism of permeability enhancement predicts a statistically random sign of the water level changes if a sufficiently large number of observations are available (Wang and Chia, 2008), consistent with our data. Analyses of the tidal response to the Wenchuan earthquake in some near-field wells also show permeability enhancement following the Wenchuan earthquake (Lai et al., 2013). Thus the hypothesis of permeability changes induced by dynamic stress produced by seismic waves may be valid not only in the intermediate-field, but also in the near-field.

6.2. Liquefaction occurrence

The maximum distance to liquefaction sites for the Wenchuan earthquake is about ten times larger than that for the Lushan earthquake, and the minimum seismic energy density required to trigger liquefaction is only 1/20 of the latter. The needed seismic energy density or amplitude of ground motion should be similar for the two earthquakes because the earthquakes had similar focal mechanisms and similar geology (neglecting complexities such as topographic gradients). One possibility is that the frequency contents of the ground motions are different, with more energy at longer periods for the larger Wenchuan earthquake. Indeed, several studies suggest that long period waves are more effective at triggering responses (Ghosh and Madabhushi, 2003; Kostadinov and Towhata, 2002; Rudolph and Manga, 2012; Wong and Wang, 2007). Another possibility is that the large ground shaking caused by the Wenchuan earthquake in the near-field led to changes in the surface soil properties as well as hydrogeological properties (such as permeability) of the groundwater system, reducing

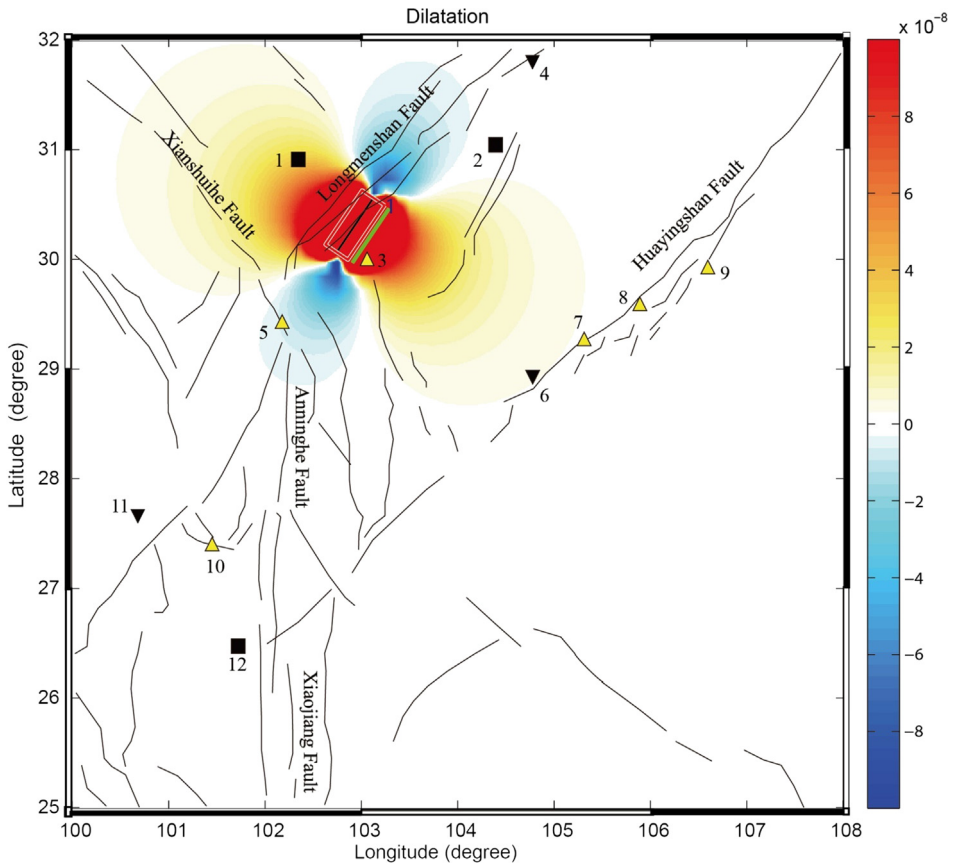

Fig. 5b. Co-seismic water level changes and co-seismic strain field distribution, following the Lushan earthquake, calculated from the fault dislocation model. Symbols in the figure have the same meaning as in Fig. 5a.

Table 3
Comparison of estimated and observed water level changes after the two earthquakes.

Well number	Wenchuan earthquake				Lushan earthquake			
	A_s [mm/10^{-9}]	Volumetric strain	Estimated WL [m]	Observed WL [m]	A_s [mm/10^{-9}]	Volumetric strain	Estimated WL [m]	Observed WL [m]
4	0.33	5.70E−06	−1.89	−9.188	0.6	−7.90E−10	4.70E−04	−0.005
5	0.76	−1.50E−07	0.11	0.269	1.69	−1.10E−08	1.80E−02	0.14
6	0.49	4.90E−08	−0.02	−1.1	0.43	3.20E−09	−1.40E−03	−0.752
7	0.16	1.60E−07	−0.03	−0.92	0.16	2.30E−09	−3.60E−04	0.1
8	0.8	2.10E−07	−0.16	−0.68	0.45	1.80E−09	−7.90E−04	0.101
9	0.68	2.30E−07	−0.15	−0.95	0.63	9.10E−10	−5.70E−04	0.042
11	0.72	−2.80E−08	0.02	0.034	0.8	−3.00E−10	2.40E−04	−0.086
12	0.36	−2.80E−08	0.01	0.05	0.18	−1.50E−10	2.80E−05	–

Note: WL stands for the Water level.

the susceptibility to liquefaction. Hydrological systems appear to recover with time, with time scales from minutes (Elkhoury et al., 2011; Geballe et al., 2011) to months (Elkhoury et al., 2006; Xue et al., 2013) and to several years (Claesson et al., 2004; Claesson et al., 2007; Davis et al., 2001; Kitagawa et al., 2007; Manga and Rowland, 2009). Thus, the effects of the Wenchuan earthquake on the regional hydrological systems may have not completely recovered during the 5-year interval between the two earthquakes.

7. Conclusions

We test proposed mechanisms for earthquake-induced hydrological changes by using data from two earthquakes that occurred on the same fault zone and had similar focal mechanisms. We show that the static strain hypothesis cannot be the dominant mechanism either in the near-field or in the intermediate-field, while the permeability enhancement hypothesis passes the test. We also show that there are significant differences in the liquefaction response to the two events. The minimum seismic energy required to trigger liquefaction during the first earthquake is ~1/20 of that required for the second, suggesting either that liquefaction is more sensitive to low seismic frequencies or that the effects of the Wenchuan earthquake on the regional hydrological system had not completely recovered after the 5-year interval between the two earthquakes.

Acknowledgements

We thank Chunguo Liu and Xianhe Yang for providing the groundwater level data. This research is supported by National Natural Science Foundation of China (Grant 40930637), the Special Project of Seismological Community (2008419079), the Specialized Research Fund for the Doctoral Program of Higher Education of China (20100022110001), Fundamental Research Funds for the Central Universities (2652013088), the China Scholarship Council,

and the US National Science Foundation. We thank two reviewers for comments and suggestions.

References

Brodsky, E.E., Roeloffs, E., Woodcock, D., Gall, I., Manga, M., 2003. A mechanism for sustained groundwater pressure changes induced by distant earthquakes. J. Geophys. Res. 108, 2390.

Burbey, T.J., 2010. Fracture characterization using Earth tide analysis. J. Hydrol. 380, 237–246.

Cao, Z., Yuan, X., Chen, L., Sun, Y., Meng, F., 2010. Summary of liquefcation macrophenomena in Wenchuan earthquake. Chin. J. Geotechn. Eng. 32, 645–650 (in Chinese).

Claesson, L., Skelton, A., Graham, C., Dietl, C., Mörth, M., Torssander, P., Kockum, I., 2004. Hydrogeochemical changes before and after a major earthquake. Geology 32, 641–644.

Claesson, L., Skelton, A., Graham, C., Mörth, C.M., 2007. The timescale and mechanisms of fault sealing and water–rock interaction after an earthquake. Geofluids 7, 427–440.

Davis, E., Wang, K., Thomson, R., Becker, K., Cassidy, J., 2001. An episode of seafloor spreading and associated plate deformation inferred from crustal fluid pressure transients. J. Geophys. Res. 106, 21953–21963.

Doan, M.-L., Brodsky, E.E., Prioul, R., Signer, C., 2006. Tidal analysis of borehole pressure—A tutorial. Schlumberger Research Report. University of California, Santa Cruz.

Elkhoury, J.E., Brodsky, E.E., Agnew, D.C., 2006. Seismic waves increase permeability. Nature 441, 1135–1138.

Elkhoury, J.E., Niemeijer, A., Brodsky, E.E., Marone, C., 2011. Laboratory observations of permeability enhancement by fluid pressure oscillation of in situ fractured rock. J. Geophys. Res. 116.

Ge, S., Stover, S.C., 2000. Hydrodynamic response to strike- and dip-slip faulting in a half-space. J. Geophys. Res. 105, 25513–25524.

Geballe, Z.M., Wang, C.Y., Manga, M., 2011. A permeability change model for water-level changes triggered by teleseismic waves. Geofluids 11, 302–308.

Ghosh, B., Madabhushi, S., 2003. A numerical investigation into effects of single and multiple frequency earthquake motions. Soil Dyn. Earthq. Eng. 23, 691–704.

Huang, F., Jian, C., Tang, Y., Xu, G., Deng, Z., Chi, G.-C., Farrar, C.D., 2004. Response changes of some wells in the mainland subsurface fluid monitoring network of China, due to the September 21, 1999, Ms7.6 Chi-Chi earthquake. Tectonophysics 390, 217–234.

Institute of Geophysics – CAS (China Earthquake Administration), 1976. China Earthquake Catalog. Center for Chinese Research Material, Washington, DC (in Chinese).

Itaba, S., Koizumi, N., Toyoshima, T., Kaneko, M., Sekiya, K., Ozawa, K., 2008. Groundwater changes associated with the 2004 Niigata-Chuetsu and 2007 Chuetsu-oki earthquakes. Earth Planets Space 60, 1161.

Jónsson, S., Segall, P., Pedersen, R., Björnsson, G., 2003. Post-earthquake ground movements correlated to pore-pressure transients. Nature 424, 179–183.

Kitagawa, Y., Fujimori, K., Koizumi, N., 2007. Temporal change in permeability of the Nojima fault zone by repeated water injection experiments. Tectonophysics 443, 183–192.

Kostadinov, M., Towhata, I., 2002. Assessment of liquefaction-inducing peak ground velocity and frequency of horizontal ground shaking at onset of phenomenon. Soil Dyn. Earthq. Eng. 22, 309–322.

Lai, W.-C., Hsu, K.-C., Shieh, C.-L., Lee, Y.-P., Chung, K.-C., Koizumi, N., Matsumoto, N., 2010. Evaluation of the effects of ground shaking and static volumetric strain change on earthquake-related groundwater level changes in Taiwan. Earth Planets Space 62, 391–400.

Lai, G., Ge, H., Xue, L., Brodsky, E.E., 2013. Tidal response variation and recovery following the Wenchuan earthquake from water level data of multiple wells in the near field. Tectonophysics. http://dx.doi.org/10.1016/j.tecto.2013.08.039.

Lin, J., Stein, R.S., 2004. Stress triggering in thrust and subduction earthquakes and stress interaction between the southern San Andreas and nearby thrust and strike-slip faults. J. Geophys. Res. 109, B02303.

Liu, Y., Huang, R., 2013. Seismic liquefaction and related damage to structures during the 2013 Lushan Mw6. 6 earthquake in China. Disabil. Advis. 6, 55–64.

Liu, C.L., Zheng, Y., Ge, C., Xiong, X., Xu, H.Z., 2013. Rupture process of the M7.0 Lushan earthquake, 2013. Sci. China Earth Sci. 56, 1178–1192.

Manga, M., Rowland, J.C., 2009. Response of Alum Rock springs to the October 30, 2007 Alum Rock earthquake and implications for the origin of increased discharge after earthquakes. Geofluids 9, 237–250.

Manga, M., Brodsky, E.E., Boone, M., 2003. Response of streamflow to multiple earthquakes. Geophys. Res. Lett. 30, 1214.

Muir-Wood, R., King, G.C., 1993. Hydrological signatures of earthquake strain. J. Geophys. Res. 98, 22035–22068.

Okada, Y., 1985. Surface deformation due to shear and tensile faults in a half-space. Bull. Seismol. Soc. Am. 75, 1135–1154.

Roeloffs, E.A., 1996. Poroelastic techniques in the study of earthquake related hydrologic phenomena. Adv. Geophys. 37, 135–195.

Roeloffs, E.A., 1998. Presistent water level changes in a well near Parkfield, California, due to lacal and distant earthquakes. J. Geophys. Res. 103, 868–889.

Rojstaczer, S., Wolf, S., Michel, R., 1995. Permeability enchancement in the shallow crust as a cause of earthquake-induced hydrological changes. Nature 373, 237–239.

Rudolph, M., Manga, M., 2012. Frequency dependence of mud volcano response to earthquakes. Geophys. Res. Lett. 39, L14303.

Shi, Z., Wang, G., Liu, C., 2013. Co-seismic groundwater level changes induced by the May 12, 2008 Wenchuan earthquake in the near field. Pure Appl. Geophys. 170, 1773–1783.

Sil, S., Freymueller, J.T., 2006. Well water level changes in Fairbanks, Alaska, due to the great Sumatra-Andaman earthquake. Earth Planets Space 58, 181–184.

Tamura, Y., Sato, T., Ooe, M., Ishiguro, M., 1991. A procedure for tidal analysis with a Bayesian information criterion. Geophys. J. Int. 104, 507–516.

Toda, S., Stein, R.S., Richards-Dinger, K., Bozkurt, S.B., 2005. Forecasting the evolution of seismicity in Southern California: Animations built on earthquake stress transfer. J. Geophys. Res. 110, B05S16.

Wakita, H., 1975. Water wells as possible indicators of tectonic strain. Science 189, 553–555.

Wang, C.-Y., 2001. Coseismic hydrologic response of an alluvial fan to the 1999 Chi-Chi earthquake Taiwan. Geology 29, 831–834.

Wang, C.-Y., 2007. Liquefaction beyond the near field. Seismol. Res. Lett. 78, 512–517.

Wang, C.-Y., Chia, Y., 2008. Mechanism of water level changes during earthquakes: Near field versus intermediate field. Geophys. Res. Lett. 35, L12402.

Wang, C.-Y., Wang, C.-H., Manga, M., 2004. Coseismic release of water from mountains evidence from the 1999 (Mw = 7.5) Chi-Chi, Taiwan earthquake. Geology 32, 769–772.

Wang, C.-Y., Chia, Y., Wang, P.-l., Dreger, D., 2009. Role of S waves and Love waves in coseismic permeability enhancement. Geophys. Res. Lett. 36, L09404.

Wang, Q., Qiao, X., Lan, Q., Jeffrey, F., Yang, S., Xu, C., Yang, Y., You, X., Tan, K., Chen, G., 2011. Rupture of deep faults in the 2008 Wenchuan earthquake and uplift of the Longmen Shan. Nat. Geosci. 4, 634–640.

Wong, A., Wang, C.-Y., 2007. Field relations between the spectral composition of ground motion and hydrological effects during the 1999 Chi-Chi (Taiwan) earthquake. J. Geophys. Res. 112.

Xu, X., Wen, X., Yu, G., Chen, G., Klinger, Y., Hubbard, J., Shaw, J., 2009. Coseismic reverse—and oblique—slip surface faulting generated by the 2008 Mw 7.9 Wenchuan earthquake, China. Geology 37, 515–518.

Xue, L., Li, H.-B., Brodsky, E.E., Xu, Z.-Q., Kano, Y., Wang, H., Mori, J.J., Si, J.-L., Pei, J.-L., Zhang, W., 2013. Continuous permeability measurements record healing inside the Wenchuan earthquake fault zone. Science 340, 1555–1559.

Yuan, X., Cao, Z., Sun, R., Chen, L., Meng, S., Dong, L., Wang, W., Meng, F., Chen, H., Zhang, J., 2009. Preliminary research on liquefaction characteristics of Wenchuan 8.0 earthquake. Chin. J. Rock. Mech. Eng. 28, 1288–1296.

Zhang, Y., Huang, F., 2011. Mechanism of different coseismic water-level changes in Wells with similar epicentral distances of intermediate field. Bull. Seismol. Soc. Am. 101, 1531–1541.

Zhang, Y., Dong, S., Hou, C., Guo, C., Yao, X., Li, B., Du, J., Zhang, J., 2013. Geohazards induced by the Lushan Ms7.0 earthquake in Sichuan province, Southwest China: Typical examples, types and distributional characteristics. Acta Geol. Sin.-Engl. Ed. 87, 646–657.